Cancer Immunology, Immunotherapy (2021) 70:497–508
https://doi.org/10.1007/s00262-020-02697-3

ORIGINAL ARTICLE

The introduction of immunosuppressor (TDO inhibitor) significantly improved the efficacy of irinotecan in treating hepatocellular carcinoma

Qingqing Liu[1,2] · Shixian Hua[1,2] · Xinyi Wang[1,2] · Feihong Chen[1,2] · Shaohua Gou[1,2]

Received: 16 June 2020 / Accepted: 11 August 2020 / Published online: 25 August 2020

Abstract

As TDO inhibitors can improve the efficacy of tumor chemotherapeutics, two TDO-targeted conjugates consisting of irinotecan (**Ir**) and a TDO inhibitor unit were designed and prepared to reverse tumor immune suppression, which could remarkably enhance antitumor activity of **Ir** by boosting cellular uptakes against TDO overexpressed HepG2 cancer cells. In vitro mechanistic studies demonstrated that compound **PVIS-Ir** and **PVIG-Ir** could arrest cell cycle at G2 phase and induce cell apoptosis by mitochondrial apoptotic pathway. Furthermore, compound **PVIS-Ir** could effectively inhibit TDO protein expression via releasing a TDO inhibitor derivative, which could also completely embed in TDO protein pocket. Further mechanism study indicated that **PVIS-Ir** could block kynurenine production and deactivate aryl hydrocarbon receptor (AHR), resulting in T-cell activation and proliferation. In vivo studies confirmed that **PVIS-Ir** could improve tumor immune microenvironment in a murine model. This combinational strategy of chemotherapy and immunotherapy can be a promising way in the treatment of hepatocellular carcinoma.

Qingqing Liu and Shixian Hua have contributed equally to this work.

Electronic supplementary material The online version of this article (https://doi.org/10.1007/s00262-020-02697-3) contains supplementary material, which is available to authorized users.

Extended author information available on the last page of the article

Graphic abstract

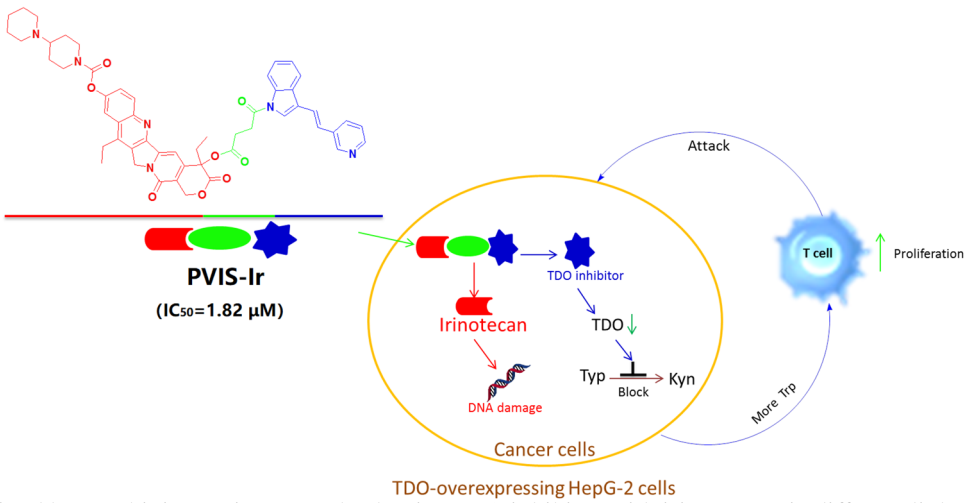

Conjugates obtained by combining an immune checkpoint TDO inhibitor with irinotecan via different linkers could improve tumor immune microenvironment by inhibiting the TDO enzyme expression to block kynurenine production and induce HepG2 cancer cell apoptosis via DNA damage through releasing a TDO inhibitor and irinotecan in cancer cells.

Keywords Chemo-immunotherapy · Tryptophan-2,3-dioxygenase (TDO) · Irinotecan · Anticancer · Hepatocellular carcinoma

Introduction

Liver cancer, the third leading cause of cancer death in the world after lung and stomach cancers, still has not had effective treatments so far, particularly in the later stage [1, 2]. Furthermore, the mortality of primary liver cancer is growing at an alarming rate [3]. Hepatocellular carcinoma (HCC), one of the most common types of primary liver cancers, is a crucial public health issue with low survival rate (about 10%) [4, 5]. The low survival rate of HCC is mainly owing to the risk factors of environment, insufficient diagnosis strategies of the tumor in the early stage, and disappointing drug development [5–7]. Up till now, it is of many difficulties to discover new therapeutic drugs to cure HCC because of the inexplicable pathological mechanisms and the complexity of liver microenvironment [5, 7]. Previous clinical tests revealed that some drugs were successful in phase II trials, but, unfortunately, they failed in phase III trials [8]. Hence, the research and development of therapeutic drugs for HCC is full of challenge.

Early research indicated that immune checkpoint inhibitors were promising for the treatment of HCC. For example, nivolumab has been approved in the US as a second-line treatment and is currently being tested with sorafenib in a phase III trial in the first-line setting [9]. It has been found that immune checkpoint inhibitors could be involved in T-cell-mediated antitumor immune response via blocking the immune checkpoint signaling pathways to boost T-cell proliferation to attack cancer cells [10, 11]. Tryptophan-2,3-dioxygenase (TDO), as a heme-containing homotetrameric enzyme encoded by TDO2 gene, is induced by glucocorticoids, tryptophan (Trp), and kynurenine (Kyn) [12, 13]. It is known to be mainly expressed in the liver to regulate the levels of systemic tryptophan and also in the brain to regulate the levels of tryptophan metabolites and 5-hydroxytryptamine [12, 14–16]. Moreover, TDO is also found expressed in many human cancers including melanoma, colorectal, hepatic, and lung cancers also express [17]. Similar to IDO (indoleamine 2,3-dioxygenase), TDO can catalyze tryptophan to produce kynurenine via the kynurenine pathway, leading to inhibiting antitumor immune response and supporting tumor cell survival [12–21]. Hence, the blockade of TDO can promote T-cell activation and proliferation and reverse tumor-associated immune resistance to kill cancer cells [21–23]. The accumulation of clinical data demonstrated that immune-based approaches for the treatment of HCC are promising, especially in combination with standard chemotherapy [9, 23–25]. However, a dual-functional strategy consisting of the potent chemotherapeutics and TDO inhibitors has not been reported so far.

In the light of above considerations, we herein present TDO-targeted conjugates (**PVIS-Ir** and **PVIG-Ir**), composed of a known TDO inhibitor (**PVI**) [13] and irinotecan (**Ir**) bridged by linkers (Fig. 1), as the immune-modulator to enhance the therapeutic effect of HCC. As a derivative of camptothecin, irinotecan is a potent DNA

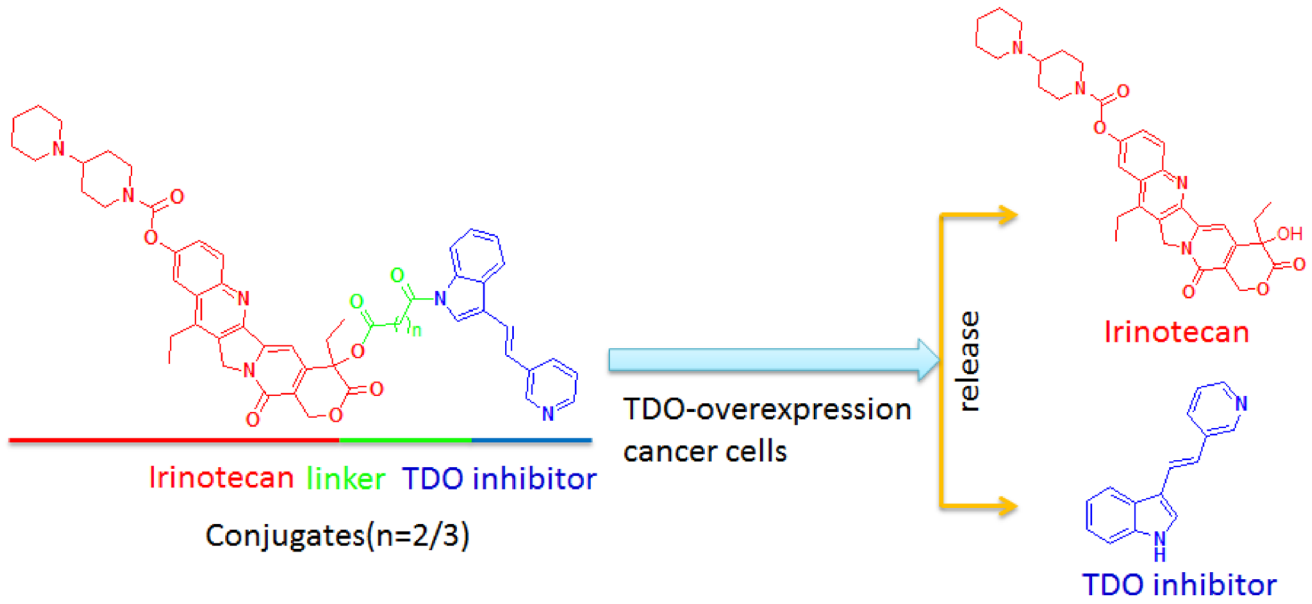

Fig. 1 Design of TDO-targeted conjugates and drug release

topoisomerase I (Top1) inhibitor that induces cancer cells apoptosis via triggering DNA damage and transcription inhibition, which is widely used in clinic as a single agent or in combined modality regimens [26–28]. A key point of our strategy is to release both **Ir** and TDO inhibitor, while the conjugate enters cancer cells to induce cancer cells apoptosis and concurrently promote T-cell proliferation via inhibiting TDO protein expression. The strategy is purposed to take advantage of the synergy between immunotherapy and chemotherapy.

Materials and methods

Chemistry

Targeted compounds (**PVIS-Ir** and **PVIG-Ir**) composed of **Ir** and TDO inhibitor derivatives (**PVIS-OH** or **PVIG-OH**) are synthesized and described in Fig. S1. The TDO inhibitor **PVI** was prepared according to the reported procedure [13, 29]. Compounds **PVIS-OH** and **PVIG-OH**, the derivates of compound **PVI**, were obtained by treatment of **PVI** with the corresponding anhydride, which has been reported elsewhere [30]. The chemical structures of the resulting conjugates **PVIS-Ir** and **PVIG-Ir** were confirmed by ^{1}H-NMR, ^{13}C-NMR, and high-resolution mass spectroscopy (HR-MS) (Supporting Information).

General tests and measurements

Compounds **PVI**, **PVIS-OH,** and **PVIG-OH** were prepared according to a literature method [13, 30]. All the chemical reagents and solvents used were of analytical grade and used without further purification, unless noted specifically. Irinotecan was purchased from Jiangsu Hengrui Pharmacetical Co., Ltd. All cancer and normal cell lines were purchased from Jiangsu KeyGEN BioTECH Company (China). ^{1}H-NMR and ^{13}C-NMR were recorded on a BRUKER AV-400/600 spectrometer with TMS as an internal standard in $CDCl_3$/DMSO-*d*6. Mass spectra were measured with an Agilent 6224 TOF LC/MS instrument. Cell cycle and apoptosis analysis were detected by flow cytometry (FAC Scan, Becton Dickenson). The cellular uptakes were detected by confocal laser scanning microscopy (CLSM) (LEICA, Germany). Peripheral blood mononuclear cells (PBMCs) from unrelated healthy donators. The anti-CD4, anti-CD8, anti-CD3, and anti-TDO2 were purchased from Biolegend for flow cytometry and western blot assay. The β-acitn, Bax, Bcl-2, cleaved caspase-3, and cleaved PAPR antibodies were purchased from Imgenex, USA.

TDO enzyme assay

The TDO enzymatic inhibitory activities were displayed as previously reported [31] and manufacturer's instructions. The TDO activity was detected via the expression level of

N-formylkynurenine by spectral analysis after treatment with compounds. In the experiment, the TDO reaction solution was added into the well of 96-well plates, and 10 µl of test inhibitor solution was added as the "Test Inhibitor", with the 10 µl same solution but without inhibitor as the "Positive Control" and "Blank". Then, 10 µl of TDO, His-tag solution (dilute TDO, His-tag in 1 × TDO Assay Buffer as 50 ng/µl solution) was added to the wells as "Positive Control", and "Test Inhibitor", and added 10 µl of 1 × TDO Assay Buffer to the well of "Blank". At last, the reaction mixtures in each well was incubated for 1.5 h at room temperature and then measured absorption at $\lambda = 323$ nm by spectral analysis.

Cell culture

HepG2 (human hepatoma cancer cell line) and LO2 (normal liver cells) were maintained at 37 °C in a 5% carbon dioxide atmosphere in monolayer culture in DMEM medium containing 10% fetal bovine serum (FBS), 100 mg/mL of penicillin, and 100 mg/mL of streptomycin.

MTT assay

All tested compounds were dissolved in DMSO (dimethyl sulfoxide) to a final concentration of 2 mmol/L and subsequently diluted in the culture medium. The in vitro antitumor activity of the targeted compounds was evaluated by the MTT assay. Briefly, about 5×10^4 cells/mL cells in DMEM medium with 10% FBS in each well of 96-well plates and incubated at 37 °C in 5% CO_2 overnight. Compounds at different concentrations were prepared and added to the test well, then incubated at 37 °C in a 5% CO_2 atmosphere. After 72 h, cells were stained with a 0.5 mg/mL solution of MTT and incubated for an additional 4 h. The medium was discarded, and subsequently, 100 µL of DMSO was added. The UV absorption intensity was detected with an ELISA reader at 490 nm. Cytotoxicity was determined on the percentage of cell survival compared with the negative control. The IC_{50} values were calculated by the Bliss method; all of the tests were repeated three times.

Cellular uptake test

The cellular uptakes of **Ir**, **PVIS-Ir,** and **PVIG-Ir** were detected in HepG2 cells using confocal laser scanning microcopy (CLSM). Briefly, 2×10^5 HepG2 cells were seeded in per well at 6-well plates with 1 mL of complete DMEM and incubated at 37 °C in 5% CO_2. After removing the culture medium, solutions of the targeted compounds at a concentration of 10 µM were added. After incubation for 4 h at 37 °C, the culture medium was removed, and cells were washed two times with PBS. Subsequently, the cells were fixed with 4% formaldehyde for 30 min at room temperature, and the slides were rinsed three times with PBS. Finally, the cells were treated with 0.5% Triton X solution and 100 µL of 10 µg/mL propidium iodide (PI) solution at 37 °C for 15 min, and the slides were rinsed with PBS three times. The resulting slides were mounted and observed with CLSM (OLYMPLUS, FV3000, Japan). For the PI channel, the excitation wavelength was 561 nm and the fluorescence was recorded at 600–650 nm. In the compound channel, the excitation wavelength was set as 488 nm and the fluorescence was collected at 500–580 nm.

AO/EB staining

The AO/EB dual staining was used to assess the live and apoptotic cells. The tested compounds were dissolved in DMSO at a final concentration of 2 mmol/L. The HepG2 cells were seeded into 6-well plates at the density of 2×10^6/well in 10% FBS-DMEM to the final volume of 2 mL and cultured in 5% CO_2 at 37 °C overnight. Then, the medium was removed and replaced with fresh medium plus 10% fetal bovine serum and treated with 10 µM of the tested compounds for 24 h. After treatment, the cells were harvested, suspended in PBS, and stained with 20 µL of AO/EB stain (100 mg/mL) at room temperature for 20 min. Fluorescence was read on an CLSM (OLYMPUS, FV3000, Japan). The AO was excited with 488 nm laser and the fluorescence was recorded at 500–550 nm. The EB was excited with 561 nm laser and the emission was collected at 600–650 nm.

Apoptosis analysis

Apoptosis rates were evaluated by flow cytometry analysis of Annexin V and PI staining. HepG2 cells were seeded into 6-well plates at the density of 2×10^6/well in 10% FBS-DMEM to the final volume of 2 mL and cultured in 5% CO_2 at 37 °C overnight, and then, drugs were added at a concentration of 10 µM. After incubated for 24 h, the cells were digested with trypsin and washed twice with cold PBS, and then collected and resuspended cells in binding buffer (0.1 M Hepes/NaOH (pH 7.4), 1.4 M NaCl, 25 mM $CaCl_2$) at a concentration of 1×10^6 cells/mL. To 100 µL of the solution in a 5 mL culture tube, 5 mL of FITC Annexin V (BD, Pharmingen) and 5 mL propidium iodide (PI) were added, and then, annexin-V FITC apoptosis kit was used. The cells were gently vortexed and incubated for 30 min at room temperature in the dark. The apoptosis experiment was analyzed with the system software (Cell Quest; BD Biosciences).

Cell cycle measurement

HepG2 cells with good vitality were seeded in 6-well plates and cultured overnight at 37 °C in 5% CO_2, and then, 10 µM of the tested compounds were incubated with cells. After

co-incubated for 24 h, cells were collected and washed twice with ice-cold PBS, and fixed and permeabilized with ice-cold 70% ethanol at 4 °C for 24 h. The cells were washed with ice-cold PBS and treated with 100 μg/mL RNase at 37 °C for 30 min, and finally stained with 50 μg/mL propidium iodide (PI) in the dark at 4 °C for 30 min. The cell cycle was measured by flow cytometry (FAC Scan, Becton Dickenson) using Cell Quest software and recording propidium iodide (PI) in the FL2 channel.

Western blot analysis

The HepG2 cells were seeded until the cell density reached 80%, and then cultured with 10 μM of the tested compounds for 24 h at 37 °C. After for 24 h, cells were collected, centrifuged, and washed twice with ice-cold PBS. And then, the cells were lysed in cell lysis buffer containing PMSF for 30 min, and lysates were collected by centrifugation at 4 °C for 10 min. The concentration of protein was measured by the BCA (bicinchoninic acid) protein assay reagents. Equal amounts of protein per line were separated on 12% SDS-polyacrylamide gel electrophoresis and transferred to PVDF Hybond-P membrane (GE Healthcare). Membranes were incubated with 5% skim milk in Tris-buffered saline with Tween 20 (TBST) buffer for 1 h, and then, the membranes being gently rotated overnight at 4 °C. Membranes were then incubated with primary antibodies at 4 °C overnight. Next, membranes incubated with peroxidase-labeled secondary antibodies for 2 h at 25 °C. The protein blots were detected by chemiluminescence reagent (Thermo Fischer Scientifics Ltd.). The β-actin was used as the loading control.

The level of kynurenine determined by HPLC

The determination of kynurenine level assays was performed according to literature reports [30, 32]. HepG2 cells were seeded in a 6-well plate at a density of 2×10^5 cells with 2 mL medium (containing 10% FBS, 100 U/mL penicillin, and 100 μg/mL streptomycin) for kynurenine concentration determination. After cultured with the tested compounds for 48 h, the cells (about 60% live cells for compound **PVIS-Ir**) were collected by centrifugation, and the 100 μL 20% trichloroacetic acid was added for protein precipitation. After incubated for 30 min at 50 °C, the sample was centrifuged for 10 min at $3000 \times g$ to remove the sediments, and the supernatant was analyzed by HPLC. Reversed-phase HPLC was implemented on a 250 × 4.5 mm ODS column and the HPLC profiles were recorded on UV detection at 360 nm. Mobile phase consisted of acetonitrile/water and flow rate was 1 mL/min. The samples were taken for HPLC analysis after filtration by 0.45 μm filter.

Quantitative (q)RT-PCR

The mRNA levels of TDO and AHR after treated with the targeted compounds were detected as described previously [30, 32]. HepG2 cells were collected to obtain the RNA for further analysis after treated with the targeted compounds. Total RNA isolated with the Qiagen RNAeasy kit and cDNA was synthesized with the Applied Biosystems reverse-transcription-kit (Foster City, CA, USA). (q)RT-PCR was performed in a Lightcycler 480 II thermocycler with SYBR Green PCR Mastermix (Roche). All primers were separated by at least one intron on the genomic DNA to exclude its amplification. PCR reactions were checked by including no-RT controls, by omission of templates, and by melting curves. Standard curves were generated for each gene. The relative quantification of gene expression was determined by the comparison of threshold values. All samples were analyzed in duplicate at two different dilutions. All results were normalized to GAPDH.

Primer sequences were (5′–3′ forward, reverse):

TGTTGCCATCAATGACCCCTT; CTCCACGACGTACTCAGCG (GAPDH)

GGCCGTGTCGATGTATCAGT; GCCTGGCAGTACTGGATTGT (AHR)

CGGTGGTTCCTCAGGCTATC; CTTCGGTATCCAGTGTCGGG (TDO)

Molecular modeling

All the docking studies were performed using Sybyl-X 2.0 on a Windows workstation. The initial coordinates for TDO were taken from the crystal structure of TDO in complex with TDO inhibitor (PDB code 2NW8) [11, 13]. The docking studies were performed on the synthetic compounds **PVIS-OH**, **PVIS-Ir**, and the parent compound **PVI**. The 3D structures of three compounds were built using Sybyl-X 2.0 sketch and then energy minimization by the MMFF94 force field and Gasteiger-Marsili charges. Then, the Powell's method was used to optimize the geometry with a distance-dependent dielectric constant and a termination energy gradient of 0.05 kcal/mol. After extracted the natural ligand and removed the water molecules from the crystal structure, the docking was processed. All the compounds were automatically docked into the TDO binding pocket by an empirical scoring function and a patented search engine in the surflex docking program. The protein was prepared using the Biopolymer module implemented in Sybyl. The automated docking manner was applied in the present work.

T-cell proliferation analysis

A mixed leukocyte reaction (MLR) was carried out to analyze T-cell proliferation as described previously [30, 32]. HepG2

cells were seeded in 6-well plates with a density of 1×10^5 cells/well. After cultivation for 24 h, the cells were replaced with fresh complete DMEM and treated with the tested compounds with an untreated control group. The HepG2 cells were incubated with different compounds for 2 days at 37 °C. PBMCs (2×10^5 cells/well) stained with CellTraceTM Far Red Cell Proliferation Kit (CFSE) was subsequently inserted after PHA-M stimulation. After co-culture for 6 days at 37 °C, the PBMCs were collected by centrifugation for further analysis. The cell pellets were resuspended in PBS and stained with anti-CD3 and anti-CD4/8 antibody. The T-cell proliferation was measured by flow cytometry.

Immunohistochemical analysis of immune T-cell infiltration in mouse tumor tissues

Immunohistochemical analysis was displayed on formalin-fixed and paraffin-embedded tumor sections to evaluate the levels of T-cell infiltration [33]. The BALB/c mice were supplied by Shanghai Laboratory Animal Center, China Academy of Sciences. Experimental protocols were in accordance with National Institutes of Health regulations and approved by the Institutional Animal Care and Use Committee. Briefly, the H22 (expression of TDO, not showed data) BALB/c mice model were weighed and randomly divided into different groups (three of mice in each group). Six days after 1×10^6 of H22 tumor cells were transplanted into the mice, **Ir** (10 mg/kg), **Ir/PVI** (7.2 mg/kg + 2.8 mg/kg), and compound **PVIS-Ir** (10 mg/kg) were administered to the mice by intravenous. All groups were intravenously injected via a tail vein once every 3 days, all mice were sacrificed after 9 days, and tumors were harvested to prepare tumor sections. And then, the tissue sections were rehydrated in xylene and graded alcohols after heated to 60 °C. Then, cool to room temperature after antigen retrieval in 0.1 M citrate buffer (pH 6.0) for 10 min and followed by rinsing in PBS and PBST (0.1% Tween). The tumor sections were incubated in 3% hydrogen peroxide to ablate endogenous tissue peroxidase activity. And then, the sections were incubated with primary antibodies (Abcam, Cambridge, UK) in antibody dilution buffer for 45 min at room temperature, following stained with biotinylated secondary antibody for 30 min. Images were obtained by a Leica TCS NT confocal scanner equipped with an ArKr-Laser on the Leica DM IRBE inverted microscope (lens: HCX PlanApo 63X oil/NA1.32).

Results

In vitro biological evaluation

The cytotoxic potency of compounds **PVIS-Ir** and **PVIG-Ir** was evaluated by MTT assay against HepG2 cancer cell line (hepatoma, high TDO protein expression [30]) as well as one normal cell line of LO2 (normal human liver cell), with **Ir**, **PVI**, **PVIS-OH,** and **PVIG-OH** as positive controls. The corresponding IC_{50} values were obtained following 72 h treatment and shown in Table 1 and Fig. S2. The results indicated that **PVI**, **PVIS-OH,** and **PVIG-OH** displayed insignificant cytotoxicity. It was interesting to note that compounds **PVIS-Ir** and **PVIG-Ir**, with IC_{50} values of 1.82 μM and 1.99 μM against HepG2 cancer cell line, exhibit much higher cytotoxicity than **Ir** (37.13 μM) and the mixture of **Ir/ PVI** (13.81 μM). Moreover, compounds **PVIS-Ir** and **PVIG-Ir** had low cytotoxicity against LO2 (26. 54 and 21.78 μM, respectively) in comparison with **Ir** (46.45 μM). And significantly, compound **PVIS-Ir** with a succinate linker exhibited a little better anti-proliferative activity than compound **PVIG-Ir** with a glutarate linker against the tested cancer cell lines. These in vitro results suggested that both **PVIS-Ir** and **PVIG-Ir** displayed better cell selectivity between cancer cells and normal liver cells than **Ir**.

As a conjugate containing a TDO inhibitor unit displayed the most potent cytotoxicity, the in vitro hydrolyzed behavior of **PVIS-Ir** was evaluated by HPLC in PBS (pH 5.0) at 37 °C. As noted in Fig. S3, at a weakly acidic environment (pH 5.0), free **Ir** and **PVIS-OH** were released in a time-dependent mode following the falling down peak of **PVIS-Ir**. These results indicated that **PVIS-Ir** could be hydrolyzed to release **PVIS-OH** (not **PVI**, the TDO inhibitor) and **Ir** gradually at a tumor weakly acidic environment, different from the design illustrated in Fig. 1. Hence, the TDO enzyme activity of both **PVIS-Ir** and **PVIS-OH** (the derivative of **PVI**) was evaluated with **PVI** as a control. As shown in Fig. S4, compound **PVIS-OH** and **PVIS-Ir** also displayed potent TDO inhibitory activity with IC_{50} values of 0.68 μM and 0.78 μM,

Table 1 Cytotoxic effects of compounds on human cancer and normal cell lines

Comp	IC_{50}(μM)[a]		
	HepG2	LO2	SI[b]
Ir	37.13 ± 2.20	46.45 ± 2.63	1.27
PVI	> 100	> 100	–
PVIS-OH	> 100	> 100	–
PVIG-OH	> 100	> 100	–
Ir:PVI	13.81 ± 1.03	39.85 ± 5.84	2.88
PVIS-Ir	1.82 ± 0.18	26.54 ± 1.52	14.58
PVIG-Ir	1.99 ± 0.10	21.78 ± 1.79	10.95

[a]In vitro cytotoxicity was determined by MTT assay upon incubation with the compounds for 72 h. Mean values were obtained upon three independent experiments

[b]Selectivity Index = IC_{50} (LO2)/IC_{50} (HepG2)

but a little weaker than compound **PVI** (0.22 μM). These results indicated that both compounds **PVIS-Ir** and **PVIS-OH** were effective TDO inhibitors.

Cellular uptake

Fluorescence spectroscopy study indicated that **Ir** could emit strong blue fluorescence under UV-lamp irradiation [34]. Thus, the cellular uptakes of **Ir**, **PVIS-Ir,** and **PVIG-Ir** in HepG2 cells were detected using confocal laser scanning microscopy (CLSM). After HepG2 cells were cultured with the tested compounds for 4 h, the nuclei were stained for 15 min with propidium iodide (PI), and the prepared cells were detected using CLSM. According to the merged images shown in Fig. 2a, the blue fluorescence of **Ir**, **PVIS-Ir,** and **PVIG-Ir** in the cytoplasm and nuclei of HepG2 cells were detected, proving that the compounds could be internalized in the HepG2 cells. Furthermore, the cellular fluorescence intensity of **PVIS-Ir** and **PVIG-Ir** was stronger than that of **Ir**, which could be attributed to the higher cellular uptakes of **PVIS-Ir** and **PVIG-Ir** in HepG2 cells. Hence, the superior cytotoxicity of **PVIS-Ir** and **PVIG-Ir** may be due to its enhanced accumulation in HepG2 cancer cells.

Cell cycle analysis

To further investigate the mechanism of the targeted compounds, we analyzed the cell cycle distributions in HepG2 cells by propidium iodide (PI) staining using flow cytometry after 24 h treatment with the tested compounds at 10 μM. **Ir** was used as a positive control. The results in Fig. 2b and Fig. S5 have shown that the cell cycle was significantly changed after treatment with **Ir**, the percentage of S phase increased to 34% compared with the untreated group (19%). However, after treatments with **PVIS-Ir** and **PVIG-Ir**, the cell cycle arrest changed and exhibited an obvious increase in the G2 phase from 7% (negative control) to 39% and 30%, respectively. These observations demonstrated that **PVIS-Ir** and **PVIG-Ir** mainly arrested the cell cycle at G2 phase.

Induced apoptosis

The apoptosis induced by **PVIS-Ir** in HepG2 cells was observed by flow cytometry using Annexin V and propidium iodide (PI) staining. HepG2 cells were co-incubated with compounds **PVIS-Ir** and **PVIG-Ir** at 10 μM for 24 h with **Ir** as a positive control. As shown in Fig. 2c and Fig. S6, the tested compounds displayed significantly induced cancer cell apoptosis. Specifically, the apoptotic rates of **PVIS-Ir** (65%) and **PVIG-Ir** (60%) were obviously higher than that

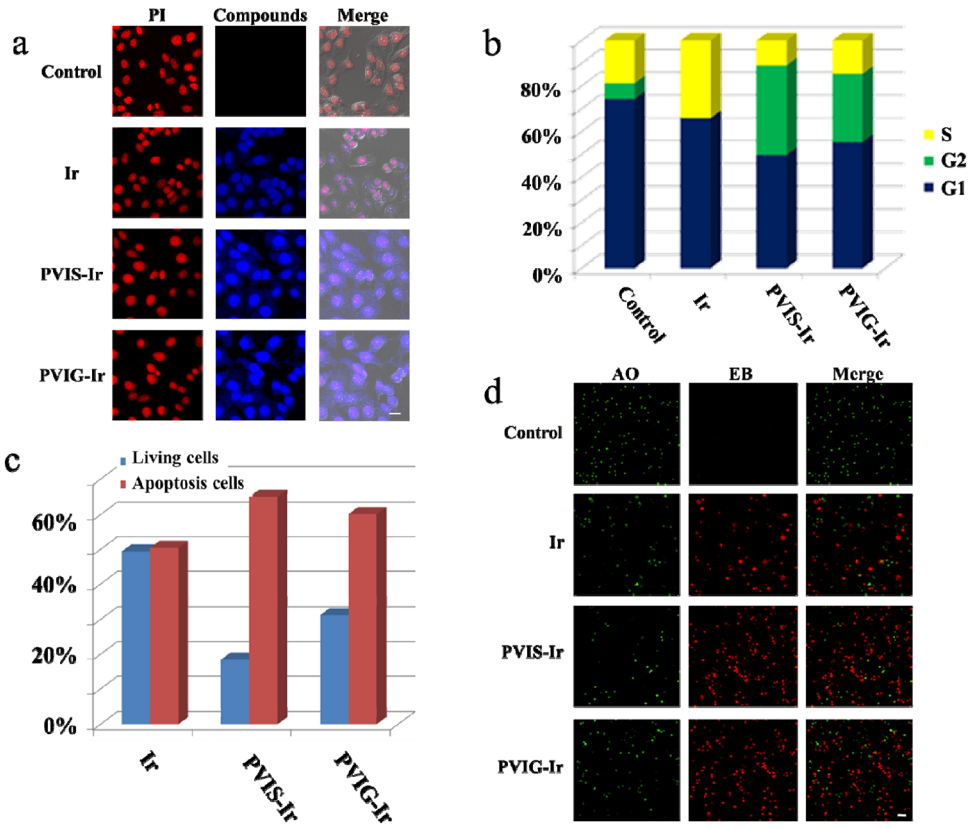

Fig. 2 Cell imaging and flow cytometry results. **a** Cellular uptakes of compounds in HepG2 cells. PI: λ_{ex} = 561 nm, λ_{em} = 600–650 nm. Compounds: λ_{ex} = 488 nm, λ_{em} = 500–580 nm. Scal bar: 20 μm. **b** Cell cycle distribution of HepG2 cells by flow cytometry analysis following the treatment of **PVIS-Ir** and **PVIG-Ir** at 10 μM for 24 h. **Ir** was used as a positive control. **c** Flow cytometry analysis for apoptosis of HepG2 cells induced by compounds at the concentration of 10 μM for 24 h. **d** AO/EB staining of compounds **Ir**, **PVIS-Ir,** and **PVIG-Ir** in HepG2 cells at 10 μM for 24 h. The live cells (green) and the apoptotic cells (red) after treatment with compounds for 24 h were exhibited. AO: λ_{ex} = 488 nm, λ_{em} = 500–550 nm. EB: λ_{ex} = 561 nm, λ_{em} = 600–650 nm. Scal bar: 100 μm

of **Ir** (50%). The results indicated that compounds **PVIS-Ir** effectively induced apoptosis superior to **Ir** and **PVIG-Ir** after treated in HepG2 cells.

AO/EB staining

Acridine orange (AO), a vital dye, can stain cell nuclei with an intact cell membrane. Meanwhile, ethidium bromide (EB) can be used to stain cells which lose their membrane integrity. To further confirm the apoptosis of HepG2 cells induced by the tested compounds, we used the AO/EB dual staining to evaluate the nuclear morphology of apoptotic cells. After treatment with the tested compounds at 10 μM for 24 h, HepG2 cells were stained with AO/EB and visualized under a fluorescence microscope. The live cells were uniformly stained as green, while the apoptotic cells were thickly stained as red. As shown in Fig. 2d, the live cells were obviously decreased and concurrently the apoptotic cells were markedly increased after treatment with the tested compounds. Both **PVIS-Ir** and **PVIG-Ir** exhibited higher apoptotic rates than **Ir**, demonstrating that the targeted compounds could induce a high quantity of apoptosis in HepG2 cells.

Compound PVIS-Ir regulates the expression of apoptosis-related proteins

To investigate the apoptotic mechanism of **PVIS-Ir** and **PVIG-Ir**, the mitochondrial apoptotic pathway-associated proteins of Bax, Bcl-2, cleaved caspase-3, and cleaved PARP were detected in HepG2 cells via western blot assay. As shown in Fig. 3a, after incubation with the tested compounds for 24 h, compounds **PVI**, **PVIS-OH,** and **PVIG-OH** displayed insignificant variation probably due to their low cytotoxicity, but different from them, compounds **PVIS-Ir** and **PVIG-Ir** showed a stronger increase on the level of Bax, a robust suppression of the level of Bcl-2 in comparsion with the control.

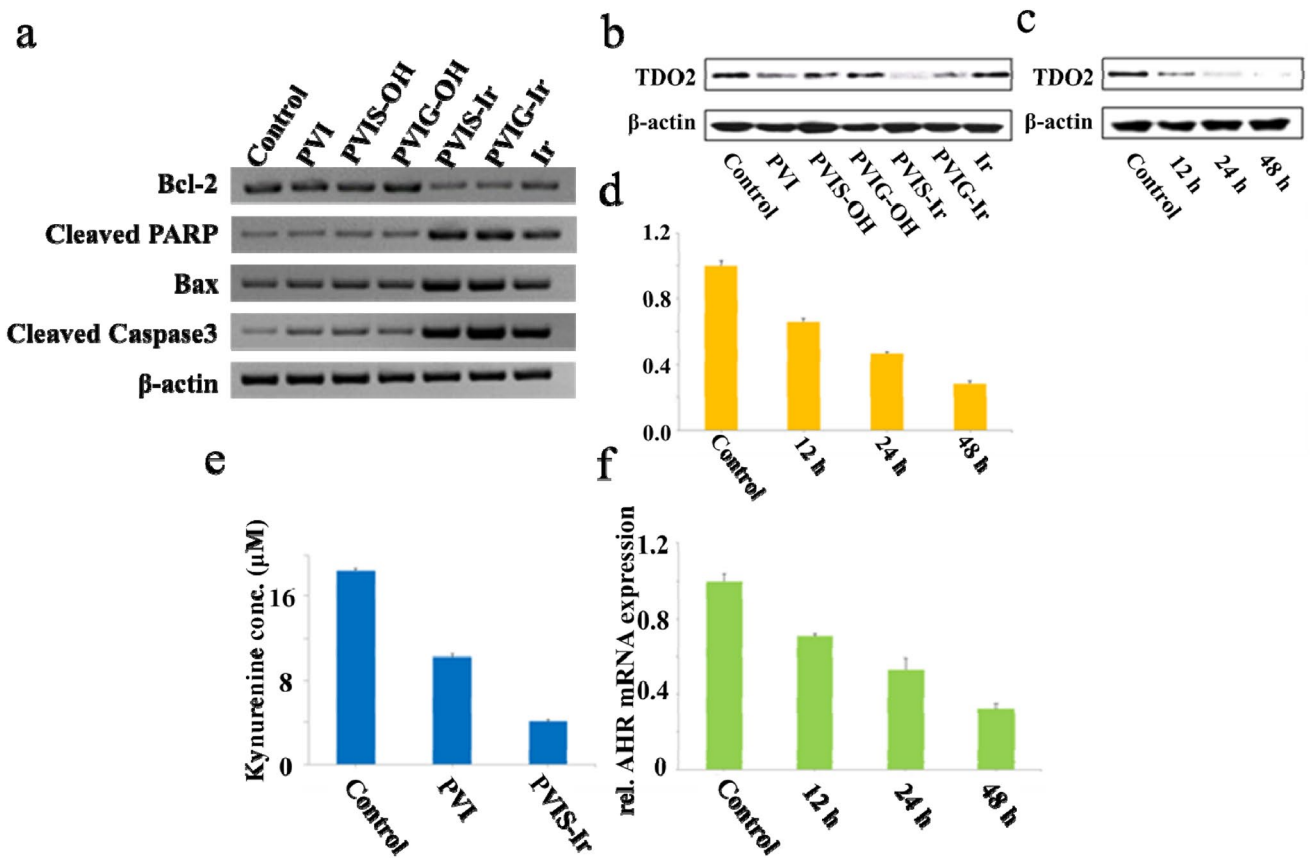

Fig. 3 The measurements of apoptosis and immune pathway. **a** Western blot results of the expression of apoptosis-related proteins after treated with the tested compounds at 10 μM for 24 h. **b** Western blot results of the pharmacological inhibition of human TDO expression in HepG2 cells after treatment with the tested compounds at 10 μM for 24 h. **c** Western blot results of the time-dependent (12, 24, and 48 h) inhibition of human TDO expression by **PVIS-Ir** in HepG2 cells. **d** qRT-PCR of time-dependent TDO mRNA after treatment with **PVIS-Ir** (10 μM). Data represent three individual experiments. **e** Kynurenine inhibition after treatment of HepG2 cells with **PVIS-Ir** (10 μM) in comparison to **PVI** and an untreated control. **f** qRT-PCR of AHR mRNA expression after treatment with **PVIS-Ir** (10 μM) for 12 h, 24 h, and 48 h. Data represent three individual experiments

Both cleaved caspase-3 and cleaved PARP were markedly up-regulated after incubation with compounds **PVIS-Ir** and **PVIG-Ir**, and the activation of caspase-3 and the cleavage of PARP could lead to cell death at last. These results indicated that compounds **PVIS-Ir** and **PVIG-Ir** could induce HepG2 cells apoptosis via a mitochondrial-mediated pathway. Besides, the **Ir** could also activate the apoptotic pathway proteins. However, the degree was smaller than that of **PVIS-Ir** or **PVIG-Ir**, indicating that the cytotoxicity of **PVIS-Ir** and **PVIG-Ir** was higher than their parent compound.

The expression of TDO in HepG2 cells

In view of the antitumor mechanism described above, the mechanism of **PVIS-Ir** and **PVIG-Ir** in immune response was also explored. As the blockade of TDO expression can promote T-cell activation and proliferation to enhance antitumor immune response [21], the capacity of **PVIS-Ir** and **PVIG-Ir** to inhibit TDO activity and protein expression in HepG2 cells were investigated. It is of significance to note in Fig. 3b that the compounds we tested exhibited effective down-regulation of TDO protein expression, except the **Ir**. Intriguingly, **PVIS-Ir** displayed the most obvious efficacy to inhibit TDO protein expression, particularly in a time-dependent manner (Fig. 3c). In addition, the level of TDO mRNA expression also displayed a remarkably time-dependent down-regulation after incubated with **PVIS-Ir** for 12, 24, and 48 h, respectively (Fig. 3d). Collectively, these results demonstrated that **PVIS-Ir** could effectively inhibit TDO protein expression, which may be due to the hydrolysis of **PVIS-Ir**.

Cell-based kynurenine inhibition assay

Since tryptophan can be degraded to kynurenine via TDO-mediated kynurenine pathway leading to cancer cell tolerance and evasion from the immune system [12, 13], we examined the capacity of **PVIS-Ir** to block kynurenine production in HepG2 cells by HPLC. The production level of kynurenine was shown in Fig. 3e. As a result, **PVI** had a better effect to block kynurenine production than the control group. Importantly, **PVIS-Ir**, which showed a stronger effect to inhibit TDO protein expression (Fig. 3b), was also much more efficient to block the kynurenine production than **PVI**. Consequently, the result confirmed that **PVIS-Ir** could block the kynurenine production via inhibiting TDO protein expression. Moreover, the inhibition of tryptophan degradation was likely to improve the cytotoxicity of the targeted compounds [35].

(q)RT-PCR of AHR mRNA expression level in HepG2 cells

The activation of aryl hydrocarbon receptor (AHR) by an endogenous ligand of kynurenine was reported to inhibit antitumor immune responses and promote cancer cell survival [22], while compound **PVIS-Ir** could block TDO protein expression resulting in the inactivation of AHR due to the inhibition of kynurenine. Thus, the mRNA of AHR in HepG2 cells was harvested for qRT-PCR after treated with **PVIS-Ir** for the appointed time. As shown in Fig. 3f, mRNA expression levels of AHR were markedly decreased in a time-dependent manner in comparison with the untreated group. This result proved that **PVIS-Ir** could interrupt the TDO-Kyn-AHR signaling pathway by inactivating the downstream of AHR.

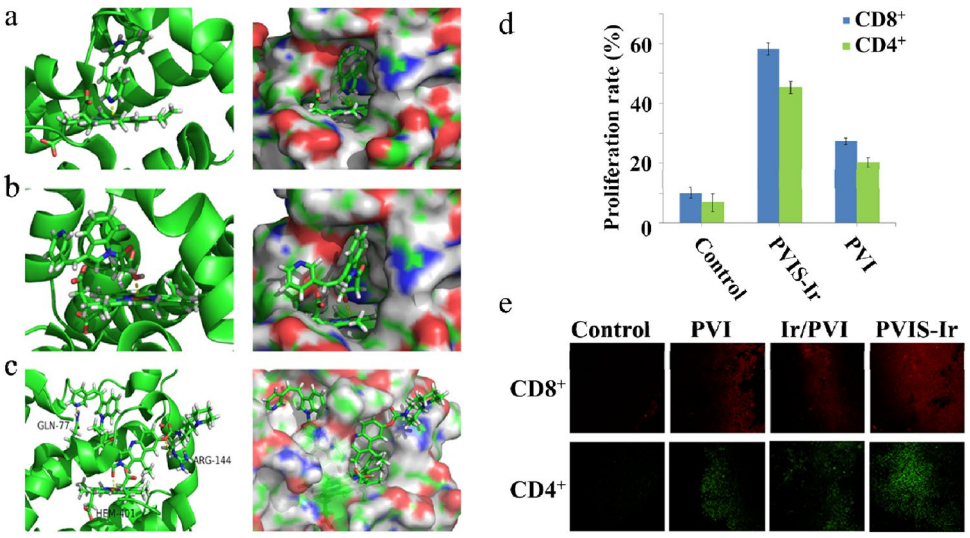

Fig. 4 Molecule docking studies and the evoke of $CD4^+$ and $CD8^+$ T cells. **a–c** Molecular modeling of **PVI**, **PVIS-OH,** and **PVIS-Ir** in complex with TDO. The binding modes and interactions of TDO with the selected compounds are as follows: **a PVI**, **b PVIS-OH**, and **c PVIS-Ir**. **d** $CD4^+$ and $CD8^+$ T-cell proliferation was estimated by the FACS analysis. Representative data of three independent experiments are presented. **e** In vivo immune response investigation after treated with various treatments: representative immunofluorescence of $CD8^+$ T cell (red) and $CD4^+$ T cell (green)

Molecular modeling

To better understand the mechanism of **PVIS-Ir** at a molecular level, molecular docking studies were performed to elucidate the binding mode of **PVIS-Ir** in the active site of TDO. To explain the different interactions of the binding mode, we also conducted the docking models of **PVI** and **PVIS-OH** as contrasts. As shown in Fig. 4a, b, and c, compounds **PVI** and **PVIS-OH** were well embedded in a pocket and made coordination and electrostatic interactions with the heme group. The significant difference between these two compounds was the pyridine moiety of **PVI** and the carbonyl group of **PVIS-OH**, which formed bonding interactions with the heme group. Exhilaratingly, in comparison with **PVI** and **PVIS-OH**, **PVIS-Ir** could well intersect the TDO pocket and form bonding interactions with the heme group, and simultaneously formed hydrogen-bonding interactions with Arg144 and Gln-77. These results indicated that compound **PVIS-Ir** can completely embed in TDO protein pocket and form hydrogen-bonding interactions, which contributes to the inhibition of TDO expression and resulting in the TDO enzyme inhibitory (Fig. S4).

Evaluate T-cell immune responses combined with compound PVIS-Ir

As the inhibition of TDO protein expression can decrease kynurenine production, leading to the improvement of antitumor immune responses with T-cell activation and proliferation [22], the cellular immune response was investigated by a mixed leukocyte reaction (MLR) in vitro. A double-staining flow cytometric assay was used to detect the proliferation of T cells. In this assay, peripheral blood mononuclear cells (PBMCs) from unrelated healthy donors, served as a mimetic immune microenvironment of body, were stimulated with a lectin of phytohemagglutinin, and then stained with a fluorescent cell staining dye of carboxyfluorescein succinimidyl ester (CFSE), and, finally, co-cultured with HepG2 cells. PBMCs were harvested after treated with the tested compounds and stained with anti-CD3/4/8 antibodies, the proliferation of T cells was assessed by flow cytometry. As shown in Fig. 4d, it was obvious that **PVI** could significantly enhance the proliferation of $CD4^+$ (20.2%) and $CD8^+$ (27.4%) T cells compared with that of the control group. Importantly, **PVIS-Ir** exhibited a much higher $CD4^+$ (45.3%) and $CD8^+$ (58.2%) T-cell proliferation rate than **PVI**. These data proved that compound **PVIS-Ir** could effectively stimulate $CD4^+$ and $CD8^+$ T-cell proliferation as an immune-chemotherapeutic agent.

IHC of the tumor tissues shows T-cell levels

Finally, we examined the role of the immune response in the tumor tissues by IHC assays with various treatments on the H22 BALB/c mice model. As shown in Fig. 4e, compared with the non-treated and irinotecan-treated groups, compound **PVIS-Ir** exhibited more infiltrated T cells ($CD4^+$ and $CD8^+$) within tumor tissues, even higher than the mixture group of **Ir** and **PVI**. These results confirmed an enhanced immunoactive microenvironment present in the tumor tissues while treated with compound **PVIS-Ir**, evidencing that the targeted compound could strengthen antitumour response via inhibiting TDO to enhance T-cell infiltration.

Conclusions

In present, we have designed and obtained two novel TDO-targeted conjugates bearing both irinotecan and a TDO inhibitor unit as immunomodulator agents to significantly boost the antitumor activity of irinotecan against HepG2 cancer cells, with the low toxicity against normal human cell line (LO2). As expected, these conjugates displayed remarkably enhanced antitumor activity of irinotecan against the TDO overexpressed HepG2 cells. Further mechanistic evaluations revealed that compound **PVIS-Ir** with effective accumulation in cancer cells exhibited a higher apoptotic rate than irinotecan and compound **PVIG-Ir** via a mitochondrial-dependent apoptotic pathway by releasing the TDO inhibitor derivative **PVIS-OH** and **Ir** at a tumor weakly acidic environment. Interestingly, **PVIS-Ir** displayed more effectively inhibition of TDO protein expression than **PVIG-Ir** and led to the decrease of Kyn production and the deactivation of downstream AHR, which may be due to the hydrolysis of **PVIS-Ir**. Molecular docking study indicated that compound **PVIS-Ir** can also contribute to the inhibition of TDO expression by fully embedding in TDO protein pocket and forming hydrogen-bonding interactions, which may result in the potent TDO enzyme inhibitory activity of **PVIS-Ir**. Further study demonstrated that treatment with **PVIS-Ir** could significantly increase the number of both $CD4^+$ and $CD8^+$ T cells. In vivo studies indicated that treatment with **PVIS-Ir** could significantly increase the numbers of total $CD4^+$/$CD8^+$ T cells in a murine. All results illustrated that **PVIS-Ir** could enhance immune response via boosting T-cell proliferation. Consequently, such an immunochemotherapeutic strategy by combining a TDO inhibitor unit with an antitumor agent as an immunomodulator to enhance antitumor immune response has a potential to promote antitumor effect in HCC therapy significantly.

Funding We are grateful to the National Natural Science Foundation of China (Grant Nos. 21571033 and 81503099) for financial aids to this work. The authors would also like to thank the Zhishan Youth Scholar Program of SEU (2242019R40045) for supplying basic facilities to our key laboratory.

Compliance with ethical standards

Conflict of interest The authors declare no conflicts of interests.

Ethics approval Experimental protocols were in accordance with National Institutes of Health regulations and approved by the Institutional Animal Care and Use Committee.

Informed consent There is no patients participating in our work.

References

1. Ferlay J, Soerjomataram I, Dikshit R (2015) Cancer incidence and mortality worldwide: sources, methods and major patterns in GLOBOCAN 2012. Int J Cancer 136:359–386
2. El-Serag B (2011) Hepatocellular carcinoma. N Engl J Med 365:1118–1127
3. Bray F, Ferlay J, Soerjomataram I, Siegel RL, Torre LA, Jemal A (2018) Global cancer statistics 2018: GLOBOCAN estimates of incidence and mortality worldwide for 36 cancers in 185 countries. CA Cancer J Clin 68:394–424
4. Lafaro KJ, Demirjian AN, Pawlik TM (2015) Epidemiology of hepatocellular carcinoma. Surg Oncol Clin N Am 24:1–17
5. Xie J, Zhang AH, Wang XJ (2017) Metabolomic applications in hepatocellular carcinoma: toward the exploration of therapeutics and diagnosis through small molecules. RSC Adv 7:17217–17226
6. Beretta L (2009) Comparative analysis of the liver and plasma proteomes as a novel and powerful strategy for hepatocellular carcinoma biomarker discovery. Cancer Lett 286:134–139
7. Lee YY, McKinney KQ, Ghosh S, Iannitti DA, Martinie JB, Caballes FR, Russo MW, Ahrens WA, Lundgren DH, Han DK, Bonkovsky HL, Hwang S (2011) Subcellular tissue proteomics of hepatocellular carcinoma for molecular signature discovery. J Proteome Res 10:5070–5083
8. Llovet JM, Rossi JZ, Pikarsky E, Sangro B, Schwartz M, Sherman M (2016) Hepatocellular carcinoma. Nat Rev Dis Primers 2:16–18
9. Greten TF, Sangro B (2018) Targets for immunotherapy of liver cancer. J Hepatol 68:157–166
10. Chang HN, Liu BY, Qi YK, Zhou Y, Chen YP, Pan KM, Li WW, Zhou XM, Ma WW, Fu CY, Qi YM, Liu L, Gao YF (2015) Blocking of the PD-1/PD-L1 interaction by a D-peptide antagonist for cancer immunotherapy. Angew Chem Int Ed 54:11760–11764
11. Sharma P, Allison JP (2015) The future of immune checkpoint therapy. Science 348:56–61
12. Wu JS, Lin SY, Liao FY, Hsiao WC, Lee LC, Peng YH, Hsieh CL, Wu MH, Song JS, Yueh A, Chen CH, Yeh SH, Liu CY, Lin SY, Yeh TK, Shih C, Ueng SH, Hung MS, Wu SY (2015) Identification of substituted naphthotriazolediones as novel tryptophan 2,3-dioxygenase (TDO) inhibitors through structure-based virtual screening. J Med Chem 58:7807–7819
13. Dolusic E, Larrieu P, Moineaux L, Stroobant V, Pilotte L, Colau D, Pochet L, Eynde BV, Masereel B, Wouters J, Frederick R (2011) Tryptophan 2,3-dioxygenase (TDO) inhibitors. 3-(2-(Pyridyl)ethenyl) indoles as potential anticancer immunomodulators. J Med Chem 54:5320–5334
14. Abdel-Magid AF (2017) Targeting the inhibition of tryptophan 2,3-dioxygenase (TDO-2) for cancer treatment. ACS Med Chem Lett 8:11–13
15. Kanai M, Funakoshi H, Takahashi H, Hayakawa T, Mizuno S, Matsumoto K, Nakamura T (2009) Tryptophan 2,3-dioxygenase is a key modulator of physiological neurogenesis and anxiety-related behavior in mice. Mol Brain 2:1–16
16. Maeta A, Fukuwatari T, Funakoshi H, Nakamura T, Shibata K (2013) Tryptophan-restriction diets help to maintain L-tryptophan homeostasis in tryptophan 2,3-dioxygenase knockout mice. Int J Tryptophan Res 6:55–65
17. Eynde BVD, Pilotte L, Plaen ED (2010) Tryptophan catabolism in cancer treatment and diagnosis. WO2010008427.
18. Uyttenhove C, Pilotte L, Theate I, Stroobant V, Colau D, Parmentier N, Boon T, Van den Eynde BJ (2003) Evidence for a tumoral immune resistance mechanism based on tryptophan degradation by indoleamine 2,3-dioxygenase. Nat Med 9:1269–1274
19. Meisel R, Zibert A, Laryea M, Gçbel U, D-ubener W, Dilloo D (2004) Human bone marrow stromal cells inhibit allogeneic T-cell responses by indoleamine 2,3-dioxygenase-mediated tryptophan degradation. Blood 103:4619–4621
20. Munn DH, Mellor AL (2007) Indoleamine 2,3-dioxygenase and tumor-induced tolerance. J Clin Invest 117:1147–1154
21. Pilottea L, Larrieua P, Stroobant V, Colau D, Dolušić E, Frédérick R, Plaen ED, Uyttenhove C, Wouters J, Masereel B, Eyndea BJV (2012) Reversal of tumoral immune resistance by inhibition of tryptophan 2,3-dioxygenase. Proc Natl Acad Sci USA 109:2497–3250
22. Opitz CA, Litzenburger UM, Sahm F, Ott M, Tritschler I, Trump S, Schumacher T, Jestaedt L, Schrenk D, Weller M, Jugold M, Guillemin GJ, Miller CL, Lehmann I, Deimling AV, Wick W, Platten M (2011) An endogenous tumour-promoting ligand of the human aryl hydrocarbon receptor. Nature 478:197–203
23. Gao H, Li K, Tu H, Pan X, Jiang H, Shi B (2014) Development of T cells redirected to glypican-3 for the treatment of hepatocellular carcinoma. Clin Cancer Res 20:6418–6428
24. Palmer DH, Midgley RS, Mirza N, Torr EE, Ahmed F, Steele JC (2008) A phase II study of adoptive immunotherapy using dendritic cells pulsed with tumour lysate in patients with hepatocellular carcinoma. Hepatology 49:124–132
25. Butterfield LH, Ribas A, Dissette VB, Lee Y, Yang JQ, Rocha PL (2006) A phase I/II trial testing immunization of hepatocellular carcinoma patients with dendritic cells pulsed with four alpha-fetoprotein peptides. Clin Cancer Res 12:2817–2825
26. Husain I, Mohler JL, Seigler HF, Besterman JM (1994) Elevation of topoisomerase I messenger RNA, protein, and catalytic activity in human tumors: demonstration of tumor-type specificity and implications for cancer chemotherapy. Cancer Rev 54:539–546
27. Pommier Y (2006) Topoisomerase I inhibitors: camptothecins and beyond. Nat Rev Cancer 6:789–802
28. Oostendorp LJ, Stalmeier PF, Pasker-de Jong PC, Van der Graaf WT, Ottevanger PB (2010) Systematic review of benefits and risks of second-line irinotecan monotherapy for advanced colorectal cancer. Anticancer Drugs 21:749–758
29. Salter M, Hazelwood R, Pogson CI, Iyer R, Madge DJ (1995) The effects of a novel and selective inhibitor of tryptophan 2,3-dioxygenase on tryptophan and serotonin metabolism in the rat. Biochem Pharmacol 49:1435–1442
30. Hua SX, Chen FH, Xu G, Gou SH (2019) Multifunctional platinum(IV) complexes as immunostimulatory agents to promote cancer immunochemotherapy by inhibiting tryptophan-2,3-dioxygenase. Eur J Med Chem 169:29–41
31. Li JS, Han Q, Fang JM, Rizzi M, James AA, Li JY (2006) Biochemical mechanisms leading to tryptophan 2,3-dioxygenase activation. Arch Insect Biochem 64:74–87

32. Awuah SG, Zheng YR, Bruno PM, Hemann MT, Lippard SJ (2015) A Pt(IV) pro-drug preferentially targets indoleamine-2,3-dioxygenase, providing enhanced ovarian cancer Immuno-chemotherapy. J Am Chem Soc 137:14854–14857
33. Lu JQ, Liu XS, Liao YP, Salazar F, Sun BB, Jiang W, Chang CH, Jiang JH, Wang X, Wu AM, Meng H, Nel AE (2017) Nano-enabled pancreas cancer immunotherapy using immunogenic cell death and reversing immunosuppression. Nat Commun 8:1–14
34. Huang P, Wang DL, Su Y, Huang W, Zhou YF, Cui DX, Zhu XY, Yan DY (2014) Combination of small molecule prodrug and nanodrug delivery: amphiphilic drug-drug conjugate for cancer therapy. J Am Chem Soc 136:11748–11756
35. Röhrig UF, Majjigapu SR, Vogel P, Zoete V, Michielin O (2015) Challenges in the discovery of indoleamine 2,3-dioxygenase 1 (IDO1) inhibitors. J Med Chem 58:9421–9437

Affiliations

Qingqing Liu[1,2] · Shixian Hua[1,2] · Xinyi Wang[1,2] · Feihong Chen[1,2] · Shaohua Gou[1,2]

✉ Feihong Chen
101011844@seu.edu.cn

✉ Shaohua Gou
2219265800@qq.com

[1] Jiangsu Province Hi-Tech Key Laboratory for Biomedical Research, Southeast University, Nanjing 211189, China

[2] Pharmaceutical Research Center and School of Chemistry and Chemical Engineering, Southeast University, Nanjing 211189, China